Journal of proteome research

Article

pubs.acs.org/jpr

Metabolic Response to Oral Microcystin-LR Exposure in the Rat by NMR-Based Metabonomic Study

Jun He,[†] Jun Chen,*[,†] Laiyan Wu,[†,‡] Guangyu Li,[†,§] and Ping Xie*[,†]

[†]Donghu Experimental Station of Lake Ecosystems, State Key Laboratory of Freshwater Ecology and Biotechnology of China, Institute of Hydrobiology, Chinese Academy of Sciences, Donghu South Road 7, Wuhan 430072, People's Republic of China

[‡]College of Chemistry and Materials Science, South-Central University for Nationalities, Wuhan 430074, China

[§]Fisheries College of Huazhong Agricultural University, Wuhan, People's Republic of China

Supporting Information

ABSTRACT: Microcystin-LR (MCLR), a potent hepatotoxin, is causing increased risks to public health. Although the liver is the main target organ of MCLR, the metabolic profiling of liver in response to MCLR in vivo remains unknown. Here, we comprehensively analyzed the metabolic change of liver and ileal flushes in rat orally gavaged with MCLR by ^{1}H nuclear magnetic resonance (NMR). Quantification of hepatic MCLR and its glutathione and cysteine conjugates by liquid chromatography−electrospray ionization−mass spectrometry (LC-ESI-MS) was conducted. Metabonomics results revealed significant associations of MCLR-induced disruption of hepatic metabolisms with inhibition of nutrient absorption, as evidenced by a severe decrease of 12 amino acids in the liver and their corresponding elevation in ileal flushes. The hepatic metabolism signature of MCLR was characterized by significant inhibition of tyrosine anabolism and catabolism, three disrupted pathways of choline metabolism, glutathione exhaustion, and disturbed nucleotide synthesis. Notably, substantial alterations of hepatic metabolism were observable even at the low MCLR-treated group (0.04 mg/kg MCLR), although no apparent histological changes in liver were observed in the low- and medium-dosed groups. These observations offered novel insights into the microcystin hepatotoxic mechanism at a functional level, thereby facilitating further assessment and clarification of human health risk from MCs exposure.

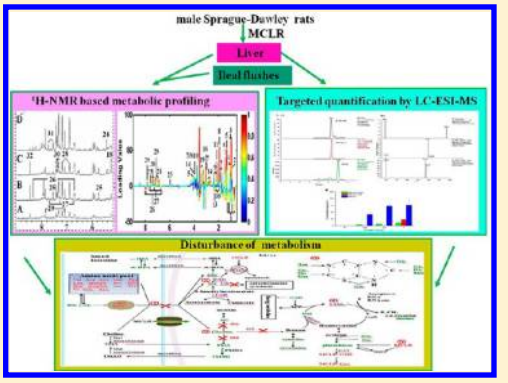

KEYWORDS: *microcystin-LR, metabonomics, NMR, glutathione, choline, nutrient absorption*

1. INTRODUCTION

Microcystins (MCs) are a family of potent hepatotoxins produced by cyanobacteria and are extensively found in freshwater (lakes, ponds, and rivers) used for drinking water sources as well as for recreational activities.[1] In recent years, MCs have caused increased risks to public health due to worldwide cyanobacterial blooms. Intoxication of animals[2−5] and human[6] following the use of MCs-contaminated water has been occurring on a global scale, and the presence of MCs in the blood of chronically exposed humans was detected.[7] Hence, MCs have gained intense scientific interest due to their ubiquitous presence and potent toxicity. To date, more than 90 analogues of MCs have been identified,[8] among which microcystine-LR (MCLR) (leucine arginine) is one of the most common and toxic variants.[9]

Previous studies have shown that MCs could strongly inhibit protein phosphatases 1 and 2A[10−12] and subsequently disturb protein phosphorylation, DNA repair, and gene expression. Meanwhile, mounting evidence suggested that MCLR stimulates the production of reactive oxygen species (ROS), followed by oxidative stress, apoptosis, and even necrosis, depending on the exposure concentration and duration.[13−15] However, MCs toxicity is a multipathway process, and the detailed mechanisms, especially the cell's systemic response as well as disruption of the downstream metabolic pathways, remain largely unknown.

Omic technologies, based on the analysis of gene transcription, protein expression, and metabolic profiles, enable a rigorous and comprehensive characterization of MCs toxicity. Especially, the metabonomic approach shows great usefulness in understanding the toxin-induced endogenous biochemical response and obtaining unbiased toxicity biomarkers.[16] Changes in metabolic phenotype can provide insight into mechanisms of toxicity and has been especially helpful in assessing preclinical toxicity.[17,18] Moreover, metabonomics have conspicuous advantages over other omic technologies (transcriptomics and proteomics). The other "omics" surveys can only evaluate the "intermediate" steps (mRNA and protein expression), and metabonomics deals with the downstream of gene and protein expression; thus, it can reveal the real cellular activities in response to MCs at a functional level.[19]

Received: July 24, 2012

dx.doi.org/10.1021/pr300685g | J. Proteome Res. XXXX, XXX, XXX−XXX

To our knowledge, there are only a few investigations of MCs effects on the metabolic profile, just one study focused on rat urine, which was part of a major academic−pharmaceutical company consortium called COMET,[17,19,20] and one study focused on the HepG2 cell line.[21] These studies identified many potent biomarkers and demonstrated that metabonomics is of great value to illustrate MCs toxicity. Nevertheless, these studies neither deeply analyzed the MCs effects on metabolic pathways nor were concerned with the metabolic profile of liver in vivo.

A number of studies have demonstrated that the liver is the primary target organ of MCs in diverse animals and humans, which induces hyperphosphorylation of proteins[10−12] and excessive ROS.[13,14] Meanwhile the liver plays a crucial role in the metabolism and detoxification of MCs through glutathione and cysteine conjugation.[22,23] However, as compared with other exemplar hepatotoxins (such as acetaminophen, carbon tetrachloride, and methapyrilene), deep and integrated analyses of the system impact on the liver and the hepatotoxicity mechanism of MCs were much less distinct. As exemplified by methapyrilene hepatotoxicity, comprehensive pathological, genomic, proteomic, and metabonomic analyses clearly revealed disruptions of genes and proteins expression levels and corresponding metabolic pathways, and the relationship between methapyrilene-induced hepatocellular necrosis and the disruption of energy metabolism was also clearly shown.[24−28] Nevertheless, information about the impact of MCs toxicity on hepatic metabolic pathways in vivo was still blank, although there already had been much hepatic genomic and proteomic information related to MCs hepatotoxicity.[15,29−33] Hence, it was an imperative need to understand the hepatic metabolic profile in response to MCs in vivo.

To better understand the hepatic metabolic response to MCs, the metabolic profile of the intestine should also be concerned, since the metabolism of toxic substances in the liver is closely linked to the intestine through absorption and enterohepatic circulation. Previous studies have shown that MCs can accumulate in the intestine[34,35] and induce apoptosis in the villi of the intestine.[36] Strong inhibition of proteins that play key roles in dietary protein digestion was also reported.[29] It seems that MCs may disturb nutritive absorption in the intestine, which subsequently affects the hepatic metabolism. For verifying this speculation, metabolic profiling of both the intestine and the liver should be investigated and analyzed integratively.

In the present study, we investigated the impact of MCLR exposure on rat via oral gavage during 7 days. Nuclear magnetic resonance (NMR) spectroscopic-based metabonomics was applied to probe dose-dependent alterations in metabolic profiles of liver extracts and ileal flushes. Multivariate data analysis of the NMR spectra was employed to uncover subtle metabolic changes after MCLR treatment. Our aims were to determine the hepatotoxic effect of MCLR on mammalian metabolic phenotypes and to identify novel hepatotoxic biomarkers for better understanding of the underlying hepatotoxic mechanism of MCLR. These results will provide novel insights into the toxicological mechanisms of MCLR at a functional level. Furthermore, the results and metabonomic approach will hold promise for further characterizing the potential risk of MCs on human health.

2. MATERIALS AND METHODS

2.1. Chemicals

MCLR was extracted and purified from freeze-dried surface blooms collected from Lake Dianchi in China with an improved Dai method.[37] Briefly, the extraction of microcystis cells was sequentially applied to an octadecylsilyl cartridge and semiprep-LC (Waters 600, United States), The content of purified MCLR was over 95%, and its identity was confirmed by liquid chromatography−electrospray ionization−mass spectrometry (LC-ESI-MS, Thermo Electron Corporation, Waltham, MA) (Figure S1 in the Supporting Information). Other materials, unless otherwise stated, were obtained from Sigma-Aldrich Ltd. (St. Louis, MO).

2.2. Animal Experiments and Sample Collection

Twenty-eight male Sprague−Dawley [Crl:CD(SD)] rats aged 6 weeks (140−150 g) were originally obtained from National Resource Center (NRLARC) for Rodent Laboratory Animal (Beijing, China). All animal experiments were conducted according to the National Institutes of Health Guide for the Care and Use of Laboratory Animals (NIH Publication No. 8023), and all efforts were made to minimize animal suffering. The rats were housed at the animal facilities of Wuhan Institute of Virology, Chinese Academy of Science, under environmentally controlled conditions (temperature, 20−22 °C; relative humidity, 40−60%; and day−night light cycle, 12−12 h). Water and food were supplied ad libitum throughout the study. After 1 week of adaptation, the rats were randomly separated into four groups of 7 rats each, including one control group and three treatment groups. The treatment groups were orally gavaged with MCLR suspended in 0.9% saline. MCLR was administered once every 2 days, totally four times at doses of 0.04, 0.2, and 1.0 mg/kg body weight/time, respectively. The high dosage selected for this study was based on a prior acute experiment.[38] The low dosage was based on the provisional World Health Organization (WHO) tolerable daily intake (TDI) of 0.04 μg/kg per person.[39] The control group was orally dosed with the vehicle (0.9% saline). On the second day after the last dose of MCLR, all rats were sacrificed. The liver was removed immediately, snap frozen, and stored at −80 °C for subsequent processing. Ileal flushes were obtained by washing the ileal lumen with 1.5 mL of a phosphate buffer solution (0.2 M Na_2HPO_4/0.04 M NaH_2PO_4, pH 7.4) using a 2 mL sterile syringe. Samples were retrieved in Eppendorf tubes, snap-frozen, and stored at −80 °C before NMR spectroscopy analyses.

2.3. Hepatic Histopathology

To investigate the histopathological changes in the livers of MCLR-exposed rats, portions of the liver were fixed in 10% formalin, cut into 4 μm paraffin sections, embedded in paraffin, and stained with hematoxylin and eosin (H&E) for histopathological examination under an optical microscope.

2.4. Sample Preparation for ^{1}H NMR Spectroscopy

2.4.1. Extraction of Polar and Lipophilic Metabolites from Liver Tissues. For extraction of polar metabolites from liver tissues, frozen liver tissue from the left lateral liver lobe (50 mg) was homogenized in ice/water bath after adding 500 μL of 50% acetonitrile/50% water. Then, samples were allowed to stand for 10 min on ice and subsequently were centrifuged at 10000 rpm for 10 min at 4 °C, and the supernatants were collected. This procedure was repeated three times, and the collected supernatants were lyophilized and reconstituted in

dx.doi.org/10.1021/pr300685g | J. Proteome Res. XXXX, XXX, XXX−XXX

600 μL of 0.1 M Na^+−K^+ buffer {0.001% 3-trimethylsilyl-1-[2,2,3,3-$^2H_4$] propionate (TSP), 30% deuterium oxide (D_2O), and 0.1% sodium azide (NaN_3)}. Similarly, 500 μL of a mixture of methanol−chloroform (1:3 by volume) was added to 50 mg of liver tissues for extraction of lipophilic metabolites. The extraction procedure was performed as described previously, and the collected lipophilic supernatants were lyophilized and reconstituted in a deuterated methanol/deuterated chloroform mixture (1:3 by volume). Both aqueous and lipophilic extracts were centrifuged again at 10000 rpm for 10 min at 4 °C. Finally, a total of 550 μL of aqueous and lipophilic supernatants were transferred into 5 mm NMR tubes, respectively.

2.4.2. Extraction of Metabolites from Ileal Flushes. About 60 mg of ileal flushes sample was vortexed for 30 s after adding 600 μL of 0.1 M phosphate buffer (0.001% TSP, 30% D_2O, and 0.03 M NaN_3, pH 7.38), and the mixtures were subjected to freeze−thaw treatments for three times. Subsequently, the samples were homogenized for 90 s with a tissuelyser (Qiagen, Hilden, Germany) and centrifuged at 12000 rpm for 10 min at 4 °C. The remaining residuals were further extracted once in the exact same manner mentioned previously.[40] The supernatants were collected and centrifuged again at 12000 rpm for 10 min. Aliquots of 550 μL were then pipetted into 5 mm NMR tubes.

2.5. ^{1}H NMR Spectroscopy

Both ^{1}H NMR spectra of aqueous and lipophilic liver extracts were acquired on a Bruker Advance 600 MHz spectrometer (Bruker Biospin, Germany), operating at 600.13 MHz ^{1}H frequency and a temperature of 298 K. Analysis for ileal flushes was achieved using a Bruker Advance 500 MHz spectrometer, equipped with cryogenic probe.

^{1}H NMR spectra of aqueous liver and ileal flushes extracts were acquired using a standard one-dimensional pulse sequence [recycle delay−90°−t_1−90°−t_m−90°−free induction decay (FID)] with t_m fixed at 100 ms and t_1 at 4 μs.[41] For each sample, 128 transients were collected into 32 K data points using a spectral width of 20 ppm. The water resonance was selectively presaturated during relaxation delay and mixing time and spoil gradient. For lipophilic liver extracts, a simple 90° pulse-acquire sequence was used, and total 128 transients were collected into 32768 data points, with a relaxation delay of 2 s and an acquisition time of 1.36 s. Metabolites were identified by reference to chemical shift tables and further two-dimensional NMR experiments when necessary.

2.6. NMR Data Processing and Analysis

A line-broadening function of 1 Hz was applied to all acquired FIDs prior to Fourier transformation. NMR spectra were manually corrected for phase and baseline distortion using TopSpin3.0 (Bruker Biospin, Germany). The spectra of ileal flushes and aqueous liver extracts were all referenced to TSP (δ 0.0), and integrals of buckets were divided into regions that have a width of 0.005 ppm for each segment. For ileal flushes, integrals of buckets include the range δ 0.5−9.0, among which residue water signals (δ 5.23−4.50) and buffer signals (δ 3.38−3.35 and δ 2.245−2.23) were removed. The integrals of buckets for aqueous liver extracts spectra include the range δ 0.5−9.5. For aqueous liver extracts spectra, the regions containing the water resonance (δ 5.22−4.67 and δ 4.64−4.46) and buffer resonance (δ 3.69−3.64, δ 3.385−3.34, δ 2.18−2.06, and δ 1.21−1.16) were excluded. Spectra of lipophilic liver extracts were referenced to tetramethylsilane (TMS) at δ 0.0. The integrals of buckets include the region between δ 5.6 and 0.5, and buffer regions including δ 5.22−4.08, δ 3.58−3.24, and δ 1.67−1.42 were removed. All integral regions were normalized to the total sum of the spectra before pattern recognition.

For data reduction and pattern recognition, a series of pattern recognition methods were applied using Simca-P 11.0 software (Umetrics AB, Umea, Sweden). Principle component analysis (PCA) was initially applied to the spectra data to visualize inherent clustering between control and treated classes. Orthogonal-projection to latent structure-discriminant analysis (O-PLS-DA)[42,43] models were further constructed to clarify the difference between control and MCLR-treated groups by the scale conversion method of unit variance scaling. The metabolites associated with the group separations were indicated by the loadings and coefficients in the coefficient plots calculated by back transformation of the loadings.

A statistical correlation analysis was conducted to establish potential associations between metabolites across different biological compartments. In each group, Pearson's correlation coefficients were calculated between influential metabolite relative intensities derived from different biological compartments of the same rat. Pixel maps were used to reveal and interpret the correlation patterns, and a cutoff value of 0.7 was applied to the absolute value of the coefficient $|r|$. The coefficients were color-coded (gradient of red colors for positive values and gradient of blue colors for negative values). The presence of colored pixels between specific metabolites represents a correlation (above the cutoff) between these metabolites, which may reflect functional correlations.

2.7. Quantification of MCLR and Its Metabolites

To deeply investigate the metabolic response to MCLR, especially the detoxification of MCLR, we quantitatively analyzed the hepatic MCLR and its glutathione and cysteine conjugates (MCLR-GSH and MCLR-Cys) in rat using LC-ESI-MS.

Liver samples were lyophilized, and about 0.2 g of lyophilized samples was extracted three times with 5 mL of acetic acid (0.01 M EDTA-Na_2 and 3 M Nacl) by ultrasonication for 3 min (30% amplitude, 60 W, 20 kHz) at 0 °C. Then, the mixtures were centrifuged (15000*g*, 4 °C), and the supernatant was treated by the method of Dai et al.[37] with minimodifications for the extracting and enriching MCLR and their metabolites.

Quantitative analyzes were performed on a Finnigan LC-ESI-MS system. The ESI-MS was carried out with a Finnigan LCQ Advantage MAX ion trap mass spectrometer (Thermo Electron Corporation) equipped with an atmospheric pressure ionization fitted with an electrospray ionization source (ESI) (Thermo Electron). Samples were maintained at 10 °C, and 10 μL injections were made into a 2.1 mm × 100 mm (3.5 μm) Waters XBridge C18 column (Waters Corporation, United States) maintained in an oven at 40 °C. MCLR, MCLR-GSH, and MCLR-Cys eluted under gradient conditions at a flow rate of 200 μL/min from acetonitrile:water = 25:75 to 75:25 over 20 min.

The mass spectrometer was operated in positive mode with an ESI spray voltage of 4.5 kV; a sheath gas flow rate of 20 units; auxiliary gas of 4.5 units; a multiplier voltage of −852 V; a tube lens voltage of 55 V for MCLR and 50 V for MCLR-GSH and MCLR-Cys; and a collision energy of 36% for MCLR, 24% for MCLR-GSH, and 34% for MCLR-Cys. Automatic gain control (AGC) on maximum isolation time was 300 ms, and three microscans per scan were acquired. The limit of detection was 70 ng g^{-1} DW.

dx.doi.org/10.1021/pr300685g | J. Proteome Res. XXXX, XXX, XXX−XXX

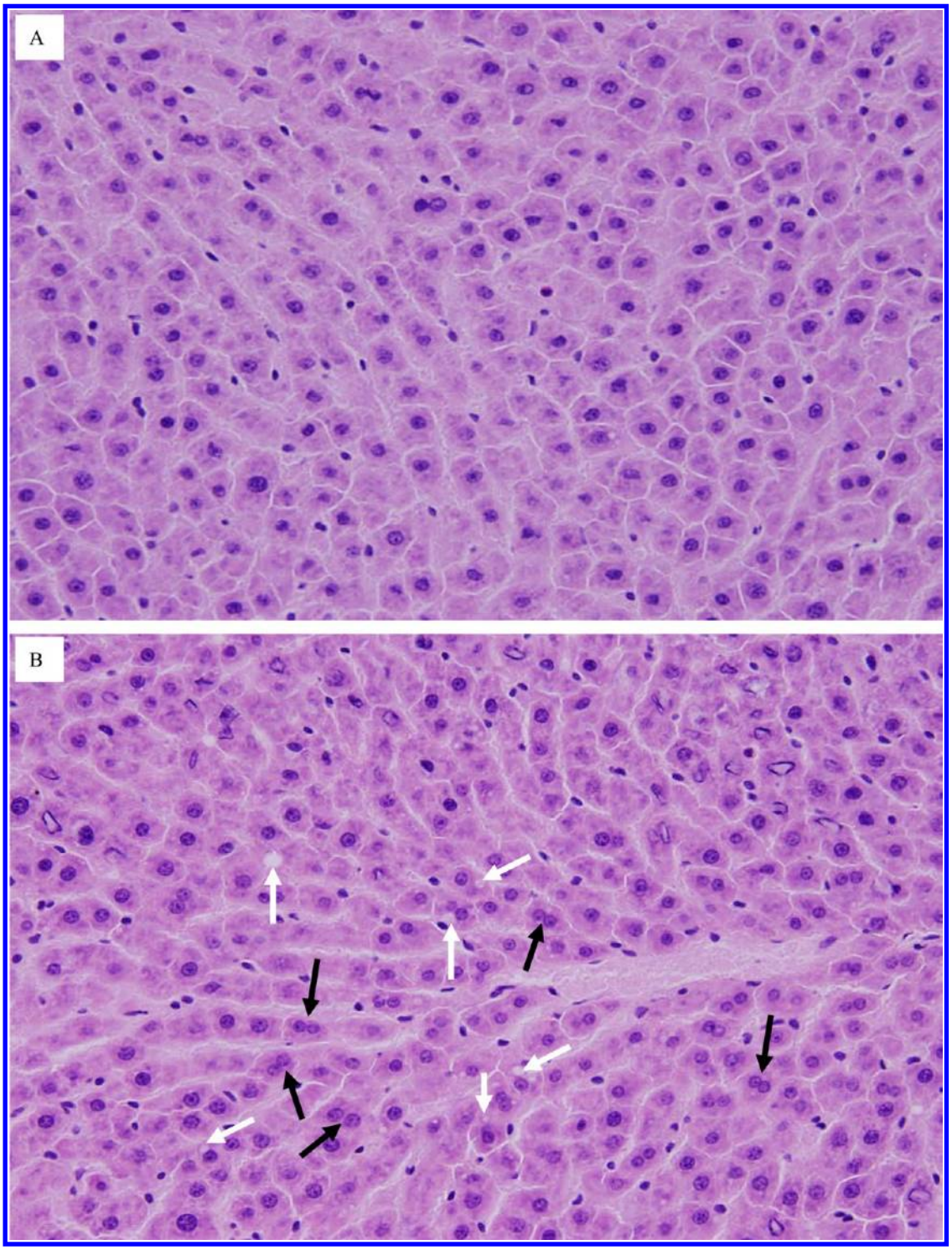

Figure 1. Light microscopy (600×) of representative sections of the liver of rats orally treated with MCLR at dose of (A) 0 mg/kg and (B) 1.0 mg/kg per 2 days. Black arrows indicate multinucleated hepatocytes, and white arrows indicate vacuoles.

3. RESULTS

3.1. Histopathology

A number of multinucleated hepatocytes as well as vacuolated hepatocytes were observed in the high-dosed group (Figure 1), implying the presence of liver injuries, while no apparent histological changes in the liver were observed in the low- and medium-dosed groups relative to the control.

3.2. ^{1}H NMR Spectroscopy and Pattern Recognition Analysis of Ileal Flushes and Liver Extracts

^{1}H NMR spectra of ileal flushes and liver extracts from control and MCLR-treated groups were dominated by numerous signals of low-molecular mass metabolites as depicted in Figures 2 and 3. The metabolite resonances were assigned based on the literature and results from 2D NMR experiments. Ileal flushes spectra were composed of mainly various amino acids, glucose, bile acids, choline, and organic acids. NMR

dx.doi.org/10.1021/pr300685g | J. Proteome Res. XXXX, XXX, XXX−XXX

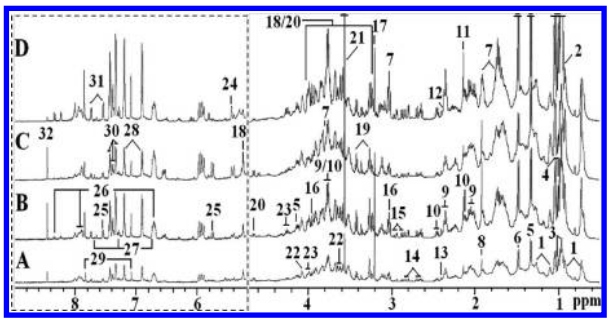

Figure 2. Representative 500 MHz ^{1}H NOESYGPPR 1D spectra (δ0.5−4.7 and δ5.2−9.0) of rat ileal flushes obtained from (A) control, (B) low-dosage, (C) medium-dosage, and (D) high-dosage groups. The region of δ5.2−9.0 (in the dashed box) was magnified four times as compared with the corresponding region of δ0.5−4.7 for the purpose of clarity. Keys: 1, bile acids; 2, leucine; 3, isoleucine; 4, valine; 5, lactate; 6, alanine; 7, lysine; 8, acetate; 9, glutamate; 10, glutamine; 11, methionine; 12, pyruvate; 13, succinate; 14, aspartate; 15, asparagine; 16, creatine; 17, choline; 18, β-glucose; 19, taurine; 20, α-glucose; 21, glycine; 22, *myo*-inositol; 23, glyceryl of lipids; 24, allantoin; 25, uracil; 26, *o*-HPA; 27, *m*-HPA; 28, tyrosine; 29, histidine; 30, phenylalanine; 31, tryptophan; and 32, formate.

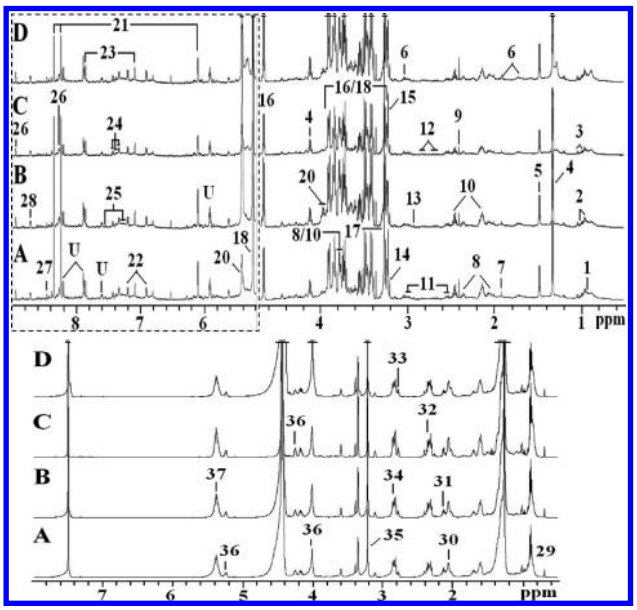

Figure 3. Representative 600 MHz ^{1}H NMR spectra of liver extracts from aquatic phase (δ0.5−4.7 and δ5.2−9.0) (top) and lipid phase (δ0.5−8.0) (bottom) obtained from (A) control, (B) low-dosage, (C) medium-dosage, and (D) high-dosage groups. The region of δ5.2−9.0 (in the dashed box) in the aquatic phase was magnified four times as compared with the corresponding region of δ0.5−4.7 for the purpose of clarity. Keys: 1, leucine; 2, isoleucine; 3, valine; 4, lactate; 5, alanine; 6, lysine; 7, acetate; 8, glutamate; 9, succinate; 10, glutamine; 11, glutathione; 12, aspartate; 13, trimethylamine; 14, choline; 15, PC; 16, β-glucose; 17, TMAO; 18, α-glucose; 19, glycine; 20, glycogen; 21, inosine; 22, tyrosine; 23, histidine; 24, phenylalanine; 25, tryptophan; 26, *N*-methylnicotinamide; 27, formate; 28, NAD; 29, HDL, cholesterol; 30, lipid, $-C\underline{H}_2-CH=CH-$; 31, NAG; 32, lipid, $-C\underline{H}_2-CO-$; 33, lipid, $=CH-C\underline{H}_2-CH=$; 34, albumin lysyl; 35, GPC; 36, glyceryl of lipids; and 37, lipid, $-C\underline{H}=C\underline{H}-$.

spectra of aqueous liver extracts were dominated by resonances from amino acids, choline metabolites, glucose, trimethylamine *N*-oxide (TMAO), and organic acids, while the NMR spectra of lipophilic liver extracts were dominated by resonances from *N*-acetyl glycoprotein signals (NAG), lipids, and glycerophosphocholine (GPC).

A series pairwise of O-PLS-DA models of ^{1}H NMR were subsequently applied to maximize the discrimination of experimental groups and to focus on metabolic variations significantly contributing to classifications. These O-PLS-DA models were constructed for each MCLR-treated group versus the control group. Characteristics of the models generated were summarized in Table 1, with high-quality goodness of fit, R^2, and high-quality goodness of predication, Q^2. Good separation of ileal flushes and aquatic and lipophilic liver extracts between control and MCLR-treated groups were achieved as shown in the O-PLS-DA scores plots (Figure 4A,D,G and Figures S2A,C,E and S3A,C,E in the Supporting Information). Using a back-scaling transformation and projection to aid biomarker visualization, metabolites significantly contributing to the separation were clearly shown in the O-PLS-DA coefficient loading plots (Figure 4B,E,H and Figured S2B,D,F and Figure S3B,D,F in the Supporting Information).[44] In these loading plots, positive peaks relative to zero represented levels of metabolites increased in the MCLR-dosed groups, whereas negative peaks indicated that levels of metabolites decreased in the MCLR-treated groups. The color of the peaks corresponded to the strength of metabolites coefficient determination (r^2), as indicated in the color scaling map on the right of the coefficient plot. A coefficient of 0.707 was used as the cutoff value for the statistical significance based on the discrimination significance at the level of p = 0.05 and degree of freedom df = 6.

MCLR significantly influenced the metabolite profiles of ileal flushes of rats. As compared with the control group, as many as 16 amino acids (Val, Tyr, Phe, Met, Lys, Leu, Ile, His, Gly, Glu, Gln, Asp, Asn, Ala, taurine, and creatine), pyruvate, lactate, acetate, and uracil increased significantly, while succinate, bile acids, *o*-hydroxyphenylacetate (*o*-HPA), and *m*-HPA decreased in the MCLR-treated groups (Table 2).

The liver metabolite profiles of rats administrated with MCLR were also markedly differentiated from rats in the control group. Levels of a range of small molecules decreased, including 12 amino acids (Val, Tyr, Phe, Lys, Leu, Ile, His, Gly, Glu, Gln, Ala, and Asp), glutathione, albumin lysyl, *N*-methylnicotinamide, nicotinamide adenine dinucleotide (NAD), inosine, choline, phosphocholine (PC)/GPC, succinate, lactate, acetate, TMAO, trimethylamine (TMA), and a putative mixture of lipids [unidentified lipids (ULP), $-CH_2-CO$: 2.14 (br), $-CH=CH-$: 5.38 (br)]. Meanwhile, the signal intensities of α-glucose, β-glucose, glycogen, and two ULP [$-CH_2-CH=CH-$: 2.02 (br), $=CH-CH_2-CH=$: 2.78 (br)] increased in MCLR-treated groups (Table 2).

3.3. Correlation Analysis of Ileal Flushes and Liver Metabolites

Correlation analysis was further applied to identify potential metabolic connections between the ileal flushes and the liver matrix (Figure 5). This analysis was carried out on groups of animals administrated with MCLR or not. Pixel maps were obtained to reveal and interpret the intra- and intermatrix correlation patterns, which highlighted the significant metabolic differences as described previously. In groups of rats administrated with MCLR, Glu/Gln in ileal flushes was positively related with Gly in ileal flushes and hepatic glucose, and it also showed negative correlation with bile acids in ileal flushes and hepatic TMAO. Meanwhile, acetate and lactate in

dx.doi.org/10.1021/pr300685g | J. Proteome Res. XXXX, XXX, XXX−XXX

Table 1. O-PLS-DA Model Summary for the Discrimination between the MCLR-Treated and the Control Groups of Ileal Flushes and Liver Extracts from NMR Data[a] Using Cross-Validation

	ileal flushes			aquatic liver extract			lipophilic liver extract		
dosage mg/kg bw	R^2X	R^2Y	Q^2Y	R^2X	R^2Y	Q^2Y	R^2X	R^2Y	Q^2Y
0.04	0.751	0.542	0.088	0.617	0.732	0.094	0.754	0.631	0.103
0.2	0.580	0.680	0.493	0.778	0.752	0.467	0.665	0.766	0.542
1.0	0.481	0.803	0.585	0.798	0.844	0.605	0.663	0.808	0.546

[a]The R^2X and R^2Y values show the total number of the variation in the X and Y matrix explained by the model, respectively. The Q^2Y value represents the predictability of the models and relates to its statistical validity.

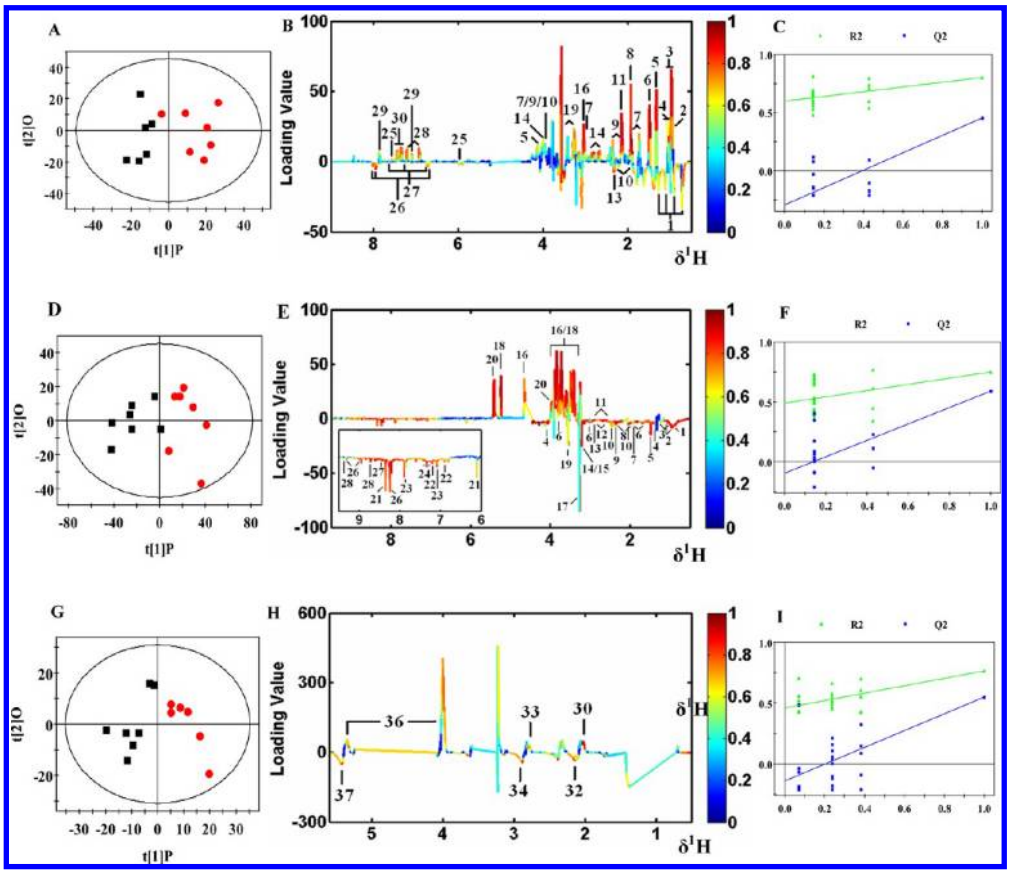

Figure 4. OPLS-DA scores plots (A, D, and G), coefficient loading plots (B, E, and H), and corresponding validation plots (C, F, and I) derived from ^{1}H NMR spectra of ileal flushes (A–C), liver aquatic extract (D–F), and liver lipophilic extract (G–I) for rats exposed to 1.0 mg/kg MCLR per 2 days. Keys of the assignments in B, E, and F are shown in Figures 2 and 3 (top and bottom), respectively.

ileal flushes together with hepatic glucose showed a positive connection with both Gly and Leu in ileal flushes, whereas bile acids were clearly negatively correlated with Gly. These metabolic associations with amino acids highlighted close functional relationships between amino acids and glucogenesis and lipid metabolism. In addition, bile acids in ileal flushes also showed a positive link to hepatic TMAO and a negative link to lactate in ileal flushes. In the liver matrix, a clear positive association between PC/GPC and TMAO was also revealed. These results suggested close correlations between hepatic lipid metabolism and intestinal activities.

3.4. Quantitative Analysis of Hepatic MCLR and Its Two Conjugates

Typical ESI LC/MS^2 spectra for MCLR and its conjugates detected in liver of a rat after MCLR exposure at 1.0 mg/kg are shown in Figure 6Aa,b. The contents of MCLR, MCLR-GSH, and MCLR-Cys in liver from the different groups are given in Figure 6B and are shown as means ± SDs. LC-ESI-MS^2 analysis showed that amounts of MCLR (RT = 11.99, m/z = 967.35, 978.21) were present in the liver, reaching as much as 91.8 ± 25.8 ng/g in the high-dose group. MCLR-GSH (RT = 10.55, m/z = 587.21, 1168.47) was also detected in all MCLR-treated groups, and its contents reached 13 ± 2 ng/g in the high-dose group. The degradation product of MCLR-GSH, namely, MCLR-Cys (RT = 10.64, m/z = 599.34, 995.41), was detected in the high-dose group, with a concentration of 28.5 ± 3.0 ng/g. These observations were in agreement with the decrease of glutathione obtained by ^{1}H NMR spectroscopy (Table 2), which suggested the conjugation of MCLR and glutathione.

4. DISCUSSION

MCs are potent hepatotoxins[45,46] and cause phosphorylation of proteins, cytoskeletal alteration, and necrosis, with a consequent hepatic hemorrhage or hepatic insufficiency.[47] However, no work to date has shown the hepatic metabolic profile disrupted by MCs in vivo. We undertook to investigate and

dx.doi.org/10.1021/pr300685g | J. Proteome Res. XXXX, XXX, XXX–XXX

Table 2. Significantly Changed Metabolites in the Ileal flushes and Liver Extracts of Rats Exposed to MCLR from NMR Data[a]

	ileal flushes			liver		
metabolites	C-L	C-M	C-H	C-L	C-M	C-H
valine	–	–	0.801	–	−0.942	−0.904
uracil	–	0.724	0.715			
tyrosine	0.841	0.747	0.797	−0.722	−0.874	−0.835
taurine	0.868	–	0.758			
succinate	–	–	−0.722	−0.786	−0.940	−0.896
pyruvate	−0.777	–	–			
phenylalanine	0.841	0.745	0.747	−0.775	−0.860	−0.873
o-HPA	−0.869	−0.715	−0.821			
m-HPA	–	–	−0.725			
methionine	0.946	0.887	0.873			
lysine	0.881	0.866	0.937	−0.820	−0.941	−0.895
leucine	0.822	–	0.859	−0.766	−0.930	−0.891
lactate	0.922	0.739	0.887	−0.802	−0.871	−0.967
isoleucine	0.833	–	0.915	–	−0.937	−0.-889
histidine	–	0.730	0.783	−0.755	−0.874	−0.878
glyceryl of lipids	0.987	–	–			
glycine	0.747	–	0.835	−0.821	−0.862	−0.928
glutamine	0.912	0.874	0.876	−0.740	−0.893	−0.859
glutamate	0.725	–	0.717	−0.771	−0.949	−0.899
creatine	0.912	0.733	0.843			
bile acids	−0.944	–	−0.733			
aspartate	0.950	0.755	0.806	−0.708	−0.950	−0.910
asparagine	0.834	0.761	–			
alanine	0.832	–	0.907	−0.726	−0.932	−0.954
acetate	0.830	0.863	0.922	−0.856	−0.927	−0.729
β-glucose				0.866	0.908	0.933
α-glucose				0.878	0.923	0.946
glycogen				0.759	0.867	0.951
TMAO				−0.812	–	−0.732
TMA				−0.870	−0.933	−0.872
N-methylnicotinamide				−0.881	−0.888	−0.906
NAD				−0.841	−0.932	−0.908
inosine				−0.803	−0.894	−0.868
GPC/PC				−0.750	−0.926	−0.841
glutathione				–	−0.914	−0.881
formate				−0.842	−0.898	−0.840
choline				−0.800	−0.939	−0.874
lipid, $-C\underline{H_2}-CO-$				−0.720	−0.825	−0.924
lipid, $-C\underline{H_2}-CH{=}CH$				–	0.774	0.917
lipid, $-CH{=}CH-$				−0.736	−0.811	−0.817
lipid, $={=}CH-C\underline{H_2}-CH{=}$				–	0.805	0.810
albumin lysyl				–	−0.771	−0.831

[a]The numbers represent the correlation coefficients of the related metabolites. Positive and negative signs indicate positive and negative correlation in the concentrations, respectively. The correlation coefficient of $|r| > 0.707$ is used as the cutoff value for the statistical significance based on the discrimination significance ($P = 0.05$, df = 6). "–" means that the correlation coefficient $|r|$ is less than 0.707. A blank of correlation coefficient means the metabolite is not detected. C, control group; L, low-dosage group; M, medium-dosage group; and H, high-dosage group.

correlate the metabolic changes in liver and ileal flushes induced by MCLR. A significant decrease of various metabolites in liver and but an opposite trend in ileal flushes was shown. This study brings the fore evidence that (i) MCLR caused absorption inhibition of nutrients, especially that of amino acids and lipids; and (ii) hepatotoxic MCLR remarkably disturbed liver metabolism including tyrosine, choline, and glutathione metabolism. (iii) Substantial alterations of hepatic metabolism were observable even at the low MCLR-treated group, suggesting a need for further assessment and clarification of the extent of the health risk through internal integration (intercompartments of organisms) and external integration (histopathology and omic technologies).

4.1. Absorption Defect of Nutrients Induced by MCLR

Nutrient absorption is the most important function of the small intestine, and the segment of ileum absorbs abundant nutrients including amino acids and lipids.[48] Meanwhile, orally administered MCLR is also mostly actively absorbed through the ileum in mammals and birds.[49−51] A high concentration of MCLR was detected in the intestine,[34,35] which may cause hazards to intestinal physiology and function. MCLR-induced gastrointestinal ailments, such as gastroenteritis, have been observed in humans.[52] Furthermore, previous studies revealed

dx.doi.org/10.1021/pr300685g | J. Proteome Res. XXXX, XXX, XXX−XXX

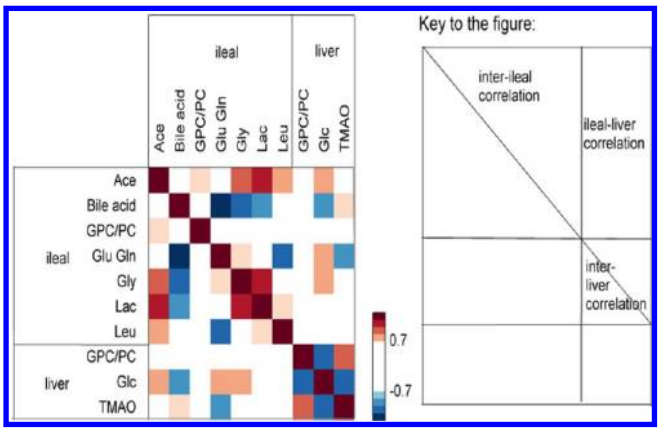

Figure 5. Integration of intermatrix metabolic correlations between ileal flushes and liver displayed by pixel maps. The absolute value of coefficient |r| 0.7 was set as the cutoff value. Pixel maps were applied to display the correlation values, in which a gradient of red colors represented positive values and a gradient of blue colors represented negative values.

that MCLR induced an increase in intestinal peroxidation level, change in the intestinal enzymes, and apoptosis in the villi of the duodenum, jejumum, and ileum in rodent models.[36,53] In spite of these studies, there is no information on whether or how the most important function of the intestine (nutrient absorption) is affected by MCs.

In the present study, the metabolite profiling of ileal flushes showed that as many as 16 amino acids in the intestinal lumen increased significantly, indicating an absorption inhibition of amino acids induced by MCLR. Correspondingly, 12 of the 16 amino acids were decreased in the liver, including four essential amino acids (Phe, Ile, Leu, and Val) (Table 2). Because essential amino acids in the liver only can be obtained from the diet and nonessential amino acids can convert each other, the decrease of various amino acids in the liver, coherent with the increase of diverse amino acids observed in intestinal lumen, further demonstrated that MCLR strikingly hindered the absorption of amino acids [Figure 7(1)]. A previous study showed that MCLR could strongly inhibit many proteins that play key roles in the digestion of dietary proteins and speculated that this inhibition potentially led to malabsorption of food substances.[29,54] The present results provided more direct evidence that the absorption of amino acids is suppressed by MCLR.

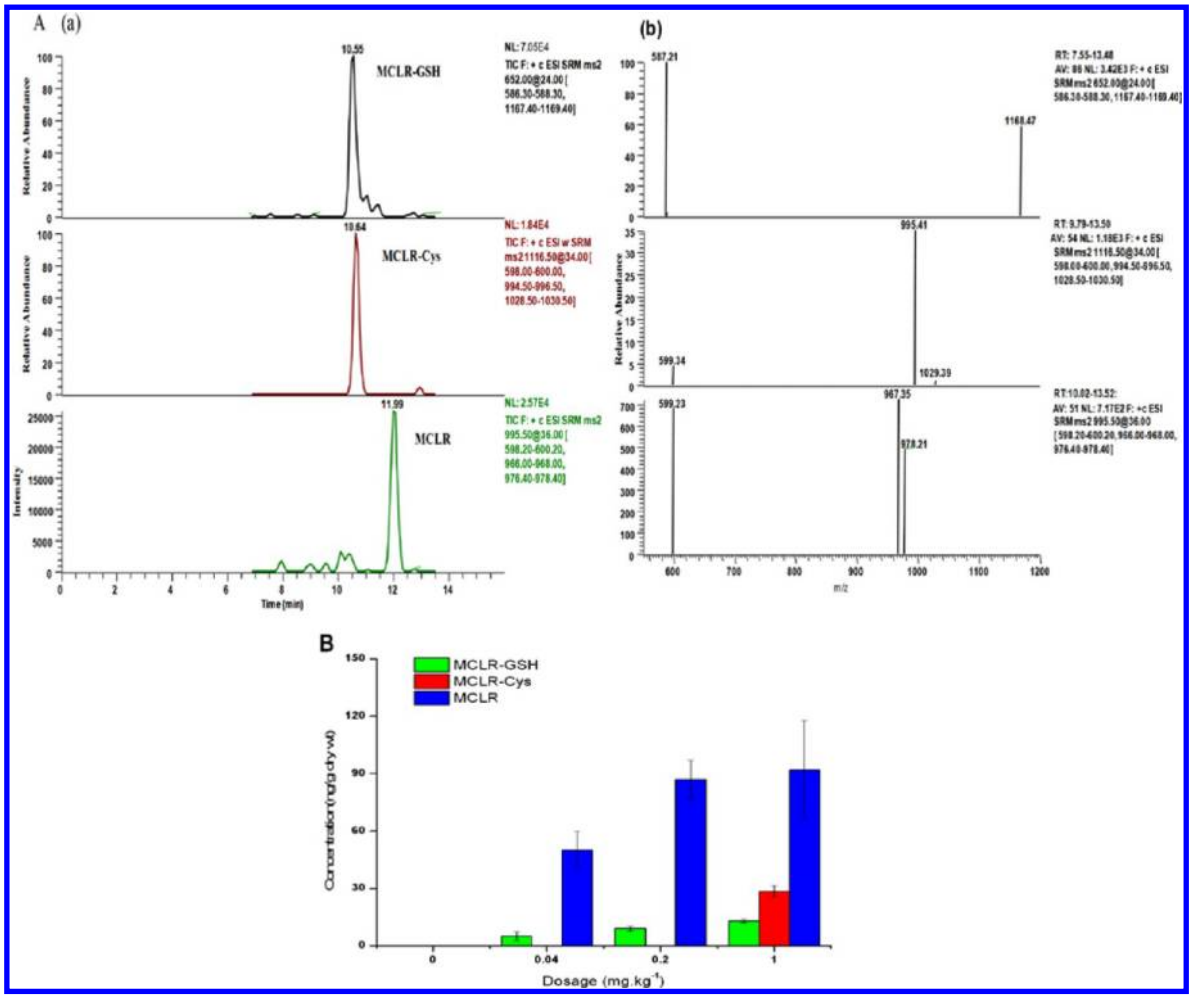

Figure 6. Quantification of MCLR and its conjugates (MCLR-GSH and MCLR-Cys) in the liver of rats dosed with 1.0 mg/kg MCLR per 2 days. (A) ESI LC/MS/MS analysis of MCLR, MCLR-GSH, and MCLR-Cys. (a) The selected reaction monitoring chromatograms for MCLR, MCLR-GSH, and MCLR-Cys. (b) The product ion mass spectrum for MCLR, MCLR-GSH, and MCLR-Cys. (B) The contents of MCLR, MCLR-GSH, and MCLR-Cys present in the livers of rats after MCLR exposure at 0, 0.04, 0.2, and 1 mg/kg.

dx.doi.org/10.1021/pr300685g | J. Proteome Res. XXXX, XXX, XXX–XXX

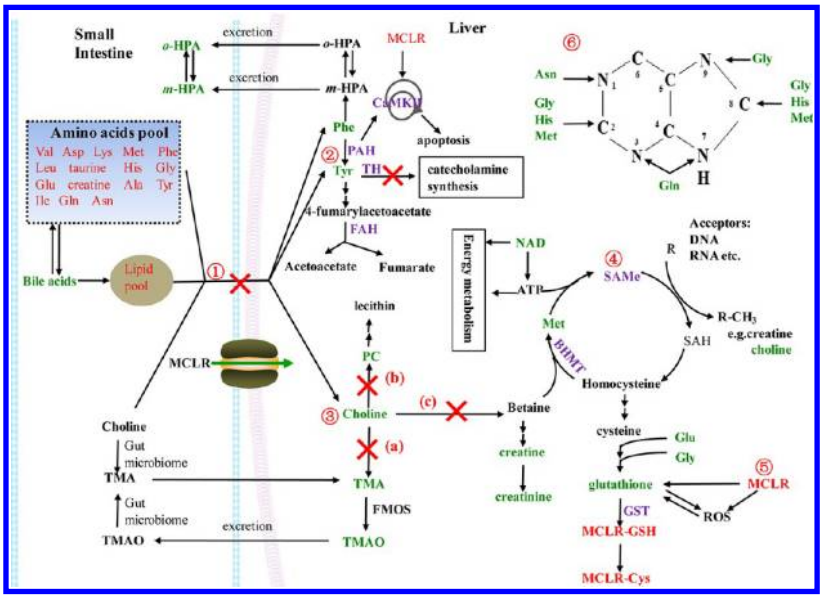

Figure 7. Most disrupted metabolic pathways in rat induced by MCLR. The number 1 represents the absorptive inhibition of nutrients, including that of amino acids, lipids, and choline; 2 represents the impaired hepatic tyrosine anabolism, catabolism, and the ensuring inhibition of catecholamine synthesis; 3a–c represents three disrupted pathways of choline metabolism; 4 and 5 represent the inhibition of glutathione synthesis and glutathione depletion due to detoxifying MCLR, respectively; and 6 indicates the disturbance in nucleotide de novo synthesis due to amino acids deficiency. The metabolites colored with green and red indicate a decrease and increase in metabolites as determined from the present metabonomic data, respectively. Substances colored with purple were previously shown to be affected by MCLR.

In our study, the absorption of lipids was also disrupted by MCLR as evidenced by the significant increase of glyceryl of lipids in ileal flushes (Table 2). Meanwhile, bile acids decreased, both taurine and glycine increased, and glycine inversely correlated with bile acids (Figure 5). As bile acids function in the solubilization and absorption of fats, cholesterol, and certain vitamins[55−57] and the conjugation of free bile acids with taurine and glycine can further enhance the solubility of lipids, the evidence obtained here implied the decreased solubilization and absorption of lipids [Figure 7(1)].

4.2. Disturbance of Multiple Hepatic Metabolisms by MCLR

In the present study, hepatotoxin MCLR remarkably disturbed liver metabolism. Significant disruption of multiple metabolic pathways included tyrosine metabolism, choline metabolism, glutathione detoxification pathways, energy metabolism, and the possible nucleotide synthesis.

4.2.1. Disruption of Hepatic Tyrosine Metabolism by MCLR. In this study, MCLR caused hepatic tyrosine depletion as evidenced by significantly decreased aromatic amino acids (Phe and Tyr) in the liver and the decreased secretion of their decomposition products *o*-HPA and *m*-HPA into the intestinal lumen. The suppressed absorption of Phe and Tyr in the intestinal lumen resulted in their low concentrations in liver [Figure 7(1)]. Furthermore, the essential amino acid Phe is the precursor of Tyr, and it always converts to Tyr in the presence of phenylalanine hydroxylase (PAH) and biopterin cofactor.[58] In the present study, the much lower concentration of Phe transported into the liver from the intestine would strikingly hinder Tyr synthesis in vivo, exacerbating the hepatic tyrosine insufficiency [Figure 7(2)]. In addition, PAH and its isoforms, the enzymes that catalyze Tyr synthesis, were previously observed to be up-phosphorylated after MCLR treatment.[33,59] PAH is the substrate of calcium-calmodulin-dependent multifunctional protein kinase II (CaMKII), which is required for MCs-induced apoptosis. So, the significantly inhibited Tyr synthesis pathway is coherent with the previously observed up-phosphorylation of PAH and the activation of CaMKII, implying the apoptosis.[60,61]

The catabolism of Tyr is also probably disrupted by MCLR. Tyr could be degraded to produce acetoacetate and fumerate. Fumaryl acetoacetate hydrolase (FAH) is the last enzyme in tyrosine catabolic pathway, catalyzing the hydrolysis of fumaryl acetoacetate into fumarate and acetoacetate.[62] Previous studies have shown the increased phosphorylation of FAH[59] and suppressed expression of homologue of FAH after exposure to MCLR.[29] Our results together with previous results indicated that the tyrosine catabolic pathway may be interrupted due to deficient material source (Phe and Tyr) and decreased enzyme activities [Figure 7(2)].

One of the most important physiological functions of tyrosine is to produce neurotransmitters catecholamine (dopamine, norepinephrine, and epinephrine). These neurotransmitters are important parts of the body's sympathetic nervous system, and their concentrations in the body directly depend upon that of tyrosine in vivo (http://www.hmdb.ca/metabolites/HMDB0015). Previous studies also showed that tyrosine hydroxylase (TH), the rate-limiting enzyme in catecholamine synthesis, catalyzing the conversion of tyrosine to 3,4-dihydroxyphenylalanine, was completely inhibited by MCs at residues ser40.[63,64] Both the present and the previous results suggested that tyrosine deficiency, disturbed by MCLR, was likely to disrupt neurotransmitters synthesis, thereby causing neuromodulation disorder [Figure 7(2)].

4.2.2. Disrupion of Hepatic Choline Metabolism by MCLR. Choline absorption and metabolism were also remarkably disrupted by MCLR. There are three major pathways utilizing dietary choline, a symxenobiotic pathway and two pure mammalian pathways.[65] Each one of these pathways seems to be interfered by MCLR in the present study. (i) Hepatic TMA and TMAO, two well-described mammalian-microbial cometabolites of choline, significantly decreased in all

dx.doi.org/10.1021/pr300685g | J. Proteome Res. XXXX, XXX, XXX–XXX

MCLR-dosed groups. TMA is derived from the gut microbial breakdown of choline and can be subsequently oxidized into TMAO via the flavine monooxygenase system (FMOS).[66,67] It seems that the reduction of TMA and TMAO in the present study was closely related to the reduced availability of choline to some bacterial strains [Figure 7(3)a]. (ii) Choline deficiency induced by MCLR in liver also led to lower circulating PC levels, an intermediate in the phosphatidycholine (lecithin) synthesis [Figure 7(3)b][66] (http://www.genome.jp/kegg-bin/show_pathway?map00564). (iii) Slight decreases of choline excretion, creatinine and creatine, were also observed in the urine of MCLR-treated rats (unpublished data) [Figure 7(3)c]. Reduction of choline in HepG2 cell exposed to MCs was also reported in a previous study.[21] Overall, the decrease in both choline and choline derivatives indicated a choline deficiency and significant disruption of choline metabolic pathways.

Choline is an essential nutrient and a basic constituent of lecithin, playing important roles in lipids metabolism. Choline deficiency has been shown to be consistently associated with hepatic steatosis[66] and atherosclerosis.[68−71] Acute choline deficiency could also cause lipid accumulation in liver, heart, and arterial tissues of rat.[72] In the present study, a significant increase of hepatic glyceryl of lipids and a putative mixture of lipids [ULP, chemical shifts: 2.02 (br), 2.78 (br)] was actually observed in MCLR-dosed rats, consistent with the increase of cholesterols and fat in HepG2 cell exposed to MC.[21] It seems that the reduced absorption and hepatic choline deficiency are important causes of the associated liver damage and cardiovascular disease induced by MCLR. Further work is need to understand the intricate relationship between the supplement of dietary choline and the metabolic phenotypes associated with MCLR-induced liver damage and to explore the preclinical drug potential of choline for reducing the MCs toxicity.

4.2.3. Exhaustion of Hepatic Glutathione Induced by MCLR. The much lower concentration of nutrients such as amino acids and choline in liver has caused interruption of hepatic glutathione synthesis. The primary source of sulfur for glutathione is *S*-adenosylmethionine (SAMe), which is the active form of Met in the SAMe trans-sulfuration pathway. In the present study, the absorption of Met in the intestine was inhibited, and hepatic choline, which provides the necessary methyl groups for Met synthesis through its intermediate betaine, was significantly decreased. These observations implied a disruption in the trans-sulfuration from SAMe to glutathione due to SAMe deficiency. Previous research detected the decreased urinary levels of SAMe after oral gavage with MCLR in SD rat using UPLC/MS.[20] Reduction in protein expression of betaine-homocysteine methyltransferase (BHMT) that catalyzes the transfer of methyl group of betaine to produce Met[73] was also detected in the liver of balb/c mice during MCLR treatment.[15] Besides the disrupted trans-sulfuration from SAMe to glutathione, the inhibited intestinal absorption of Glu and Gly, the other two precursors of glutathione, together with their lower concentration in the liver, also indicated the inhibition of glutathione synthesis [Figure 7(4)].

On the other hand, hepatic glutathione was depleted during detoxification of MCLR by conjugating with MCLR in the present study. It is known that glutathione plays an important role in the detoxification of MCs in both mammals and aquatic organisms.[22,23,35,74,75] Previous in vitro studies showed that glutathione conjugation to MCLR catalyzed by glutathione *S*-transferase (GST) is the first step to detoxify MCLR in a wide range of aquatic organisms.[23] The glutathione conjugate of MCLR (MCLR-GSH) might act as a midmetabolite and rapidly change to MCLR-Cys.[76] The biotransformation increases water solubility, reduces the toxicity, and enhances excretion of MCLR.[22,74] In the present study, amounts of MCLR and MCLR-GSH were detected in all MCLR-dosed groups, and MCLR-Cys was also detected in the high-dose group. The observations demonstrated the glutathione conjugation to MCLR for detoxification, which would lead to the glutathione depletion in liver. In addition, the rapid increase of reactive metabolites such as ROS induced by MCLR might also result in glutathione depletion.[14] Elevation in ROS due to plummeting intracellular glutathione balance after MCLR treatment was previously observed.[77] Altogether, considering the great importance of glutathione to homeostasis in vivo, glutathione depletion induced by MCLR due to inhibited synthesis and detoxification may reduce the defense ability of the organism, which results in the pathogenesis of several diseases, including liver disease, cancer, and diabetes[78] [Figure 7(5)].

4.2.4. Possible Disturbance in Nucleotide Synthesis. In the present study, the deficiency of numerous amino acids in liver may subsequently lead to disturbance in nucleotide synthesis as various kinds of amino acids play critical roles in the synthesis pathway of nucleotides. Gly, Gln, and Asn are precursors for synthesizing purine ring de novo. Meanwhile, Gly, His, Met, and formate are important sources of one carbon unit, which is also precursor of purine and pyrimidine [Figure 7(6)]. Furthermore, hepatic inosine, the precursor of nucleotide, was observed to decrease after exposure to MCLR. Increased purine oxidation product allantoin and uracil were also detected in ileal flushes (Table 2). Mikhailov et al.[79] reported that MCLR could inhibit ATP synthase in rat, and Birungi et al.[21] found that MCs caused a decrease in cyclic GMP, a component of purine metabolism and increase in cytidine diphosphate, which is converted to cytidine in the HepG2 cell line. All of these variations signified the possible disturbance of nucleotide synthesis caused by MCLR.

4.2.5. Disruption of Energy Metabolism by MCLR. Besides the notable variations mentioned above, MCLR treatment induced changes in a number of metabolites involved in energy metabolism. Significant reduction of hepatic NAD and its metabolite *N*-methylnicotinamide were first observed, suggesting NAD depletion and possible ATP depletion caused by MCLR. NAD extensively involved in glycolysis, gluconeogenesis, citric acid cycle, and cellular respiration. It serves as an electron carrier and can be converted to ATP by being alternately oxidized (NAD+) and reduced (NADH). A previous proteomic study showed that MCLR induces significant increase in protein expression of NADH dehydrogenase Fe−S protein 8 in mice.[15] *N*-Methylnicotinamide is a common form of nicotinamide elimination (http://www.hmdb.ca/metabolites/HMDB03152), and its decrease in liver may be a result of NAD depletion. Apart from NAD and *N*-methylnicotinamide, other metabolites involved in energy metabolism, such as citric acid cycle intermediate succinate and glycolysis end-product lactate, also decreased in liver.

4.3. Potential Healthy Risk of MCLR on Human

Previous subchronic toxicological studies have recorded the no observed adverse effect level (NOAEL, 0.04 mg/kg MCLR per day) in mice according to the changes of histopathological

dx.doi.org/10.1021/pr300685g | J. Proteome Res. XXXX, XXX, XXX−XXX

index and serum enzyme activity.[80] On the basis of this, with supporting data from growing pigs,[81] the WHO set a provisional TDI of 0.04 μg/kg MCLR per day for human by the incorporation of uncertainty or safety factors; consequently, the provisional guideline level for drinking water of 1 μg/L of MCLR has been determined. Nevertheless, just as Falconer and Humpage[82] pointed out, this may be revised in the light of future teratogenicity, reproductive toxicity, and carcinogenicity studies. Recent development in metabonomics shows great usefulness in understanding the toxin-induced endogenous biochemical response and obtaining unbiased toxicity biomarkers .[16]

In our study, dose−effect relationships were observed for the changes of some endogenous metabolites. Substantial alterations of hepatic metabolite profile were observed, even at the low MCLR-treated group (0.04 mg/kg MCLR), although no apparent histological changes in the liver were observed in the low- and medium-dosed groups relative to the control. As compared with the conventional histopathology, metabonomics studies enabled a more sensitive, rigorous, and comprehensive characterization of MCs toxicity in the present study. Although systemic exposures from oral doses from one species could not extrapolate directly to systemic exposure in another, results obtained from the model organism, rat, still indicated the potential healthy risk of MCLR on human. Our findings also suggest that the potential severity of MCs exposure should be further assessed and determined by integration of "conventional" histopathology and clinical pathology and the "modern" omic technologies.

5. CONCLUSIONS

In summary, the present results and analyses indicate that oral MCLR exposure induced significant disruption of metabolic pathways in rat liver. Such disruptions of hepatic metabolisms were closely related to the inhibition of nutrients absorption, especially that of amino acids and lipids. The present study offers novel insights into the toxicological mechanism of MCs at functional level, facilitating further assessment and reexamination of potential severity of MCLR intake.

■ ASSOCIATED CONTENT

Supporting Information

Figures S1−S3. This material is available free of charge via the Internet at http://pubs.acs.org.

■ AUTHOR INFORMATION

Corresponding Author

*Tel: +86-27-68780622. Fax: +86-27-68780056. E-mail: chenjun@ihb.ac.cn (J.C.) or xieping@ihb.ac.cn (P.X.).

Notes

The authors declare no competing financial interest.

■ ACKNOWLEDGMENTS

This work was funded by the National Natural Science Foundation of China (31070457). We acknowledge Beijing Nuclear Magnetic Resonance Center for use of Bruker NMR spectrometers. We thank Shanghai Sensichip infotech Co., Ltd., and Dr. Jianghua Feng of Xiamen University for help in data processing. Also, thanks to Junliang Den, HuiHui Fan, Wei Li, Luyi Liu, Jie Liu, Sujuan Zhao, Wei Zhang, Xiaochun Guo, Shangchun Li, and Yujie Wu for assistance in the animal experiment.

■ ABBREVIATIONS

MCLR, microcystine-LR; MCs, microcystins; MCLR-GSH/MCLR-Cys, glutathione and cysteine conjugate of MCLR; NOAEL, no observed adverse effect level; WHO, World Health Organization; ROS, reactive oxygen species; TDI, tolerable daily intake; TSP, 3-trimethylsilyl-1-[2,2,3,3-$^2H_4$] propionate; D_2O, deuterium oxide; NaN_3, sodium azide; TMS, tetramethylsilane; PCA, principle component analysis; O-PLS-DA, orthogonal-projection to latent structure-discriminant analysis; ESI, electrospray ionization source; AGC, automatic gain control; TMAO, trimethylamine *N*-oxide; TMA, trimethylamine; NAG, *N*-acetyl glycoprotein signals; GPC, glycerophosphocholine; PC, phosphocholine; *o*-HPA, *o*-hydroxyphenylacetate; NAD, nicotinamide adenine dinucleotide; ULP, unidentified lipids; PAH, phenylalanine hydroxylase; CaMKII, calcium-calmodulin-dependent multifunctional protein kinase II; FAH, fumaryl acetoacetate hydrolase; TH, tyrosine hydroxylase; FMOS, the flavine monooxygenase system; SAMe, *S*-adenosylmethionine; BHMT, betaine-homocysteine methyltransferase; GST, glutathione *S*-transferase; NMR, nuclear magnetic resonance; LC-ESI-MS, liquid chromatography−electrospray ionization−mass spectrometry

■ REFERENCES

(1) Chorus, I.; Falconer, I. R.; Salas, H. J.; Bartram, J. Health risks caused by freshwater cyanobacteria in recreational waters. *J. Toxicol. Environ. Health. Part B* **2000**, *3* (4), 323−347.

(2) Carmichael, W. W. Health effects of toxin-producing cyanobacteria: "The cyanohabs". *Hum. Ecol. Risk Assess.* **2001**, *7* (5), 1393−1407.

(3) DeVries, S. E.; Galey, F. D.; Namikoshi, M.; Woo, J. C. Clinical and pathologic findings of blue-green algae (*Microcystis aeruginosa*) intoxication in a dog. *J. Vet. Diagn. Invest.* **1993**, *5* (3), 403−408.

(4) Puschner, B.; Galey, F. D.; Johnson, B.; Dickie, C. W.; Vondy, M.; Francis, T.; Holstege, D. M. Blue-green algae toxicosis in cattle. *J. Am. Vet. Med. Assoc.* **1998**, *213* (11), 1605−1607 1571.

(5) Matsunaga, H.; Harada, K. I.; Senma, M.; Ito, Y.; Yasuda, N.; Ushida, S.; Kimura, Y. Possible cause of unnatural mass death of wild birds in a pond in nishinomiya, Japan: Sudden appearance of toxic cyanobacteria. *Nat. Toxins* **1999**, *7* (2), 81−84.

(6) Azevedo, S. M. F. O.; Carmichael, W. W.; Jochimsen, E. M.; Rinehart, K. L.; Lau, S.; Shaw, G. R.; Eaglesham, G. K. Human intoxication by microcystins during renal dialysis treatment in caruaru−brazil. *Toxicology* **2002**, *181−182*, 441−446.

(7) Chen, J.; Xie, P.; Li, L.; Xu, J. First identification of the hepatotoxic microcystins in the serum of a chronically exposed human population together with indication of hepatocellular damage. *Toxicol. Sci.* **2009**, *108* (1), 81−89.

(8) Ufelmann, H.; Krüger, T.; Luckas, B.; Schrenk, D. Human and rat hepatocyte toxicity and protein phosphatase 1 and 2a inhibitory activity of naturally occurring desmethyl-microcystins and nodularins. *Toxicology* **2012**, *293* (1−3), 59−67.

(9) Gupta, N.; Pant, S. C.; Vijayaraghavan, R.; Rao, P. V. L Comparative toxicity evaluation of cyanobacterial cyclic peptide toxin microcystin variants (LR, RR, YR) in mice. *Toxicology* **2003**, *188* (2−3), 285−296.

(10) Yoshizawa, S.; Matsushima, R.; Watanabe, M. F.; Harada, K.-i.; Ichihara, A.; Carmichael, W. W.; Fujiki, H. Inhibition of protein phosphatases by microcystis and nodularin associated with hepatotoxicity. *J. Cancer Res. Clin. Oncol.* **1990**, *116* (6), 609−614.

(11) Honkanen, R. E.; Zwiller, J.; Moore, R. E.; Daily, S. L.; Khatra, B. S.; Dukelow, M.; Boynton, A. L. Characterization of microcystin-

LR, a potent inhibitor of type 1 and type 2a protein phosphatases. *J. Biol. Chem.* **1990**, *265* (32), 19401−19404.
(12) Craig, M.; Luu, H. A.; McCready, T. L.; Holmes, C. F. B.; Williams, D.; Andersen, R. J. Molecular mechanisms underlying the interaction of motuporin and microcystins with type-1 and type-2a protein phosphatases. *Biochem. Cell Biol.* **1996**, *74* (4), 569−578.
(13) Jayaraj, R.; Anand, T.; Rao, P. V. L Activity and gene expression profile of certain antioxidant enzymes to microcystin-LR induced oxidative stress in mice. *Toxicology* **2006**, *220* (2−3), 136−146.
(14) Weng, D.; Lu, Y.; Wei, Y.; Liu, Y.; Shen, P. The role of ROS in microcystin-LR-induced hepatocyte apoptosis and liver injury in mice. *Toxicology* **2007**, *232* (1−2), 15−23.
(15) Chen, T.; Wang, Q.; Cui, J.; Yang, W.; Shi, Q.; Hua, Z.; Ji, J.; Shen, P. Induction of apoptosis in mouse liver by microcystin-LR a combined transcriptomic, proteomic, and simulation strategy. *Mol. Cell. Proteomics* **2005**, *4* (7), 958−974.
(16) Lindon, J. C.; Keun, H. C.; Ebbels, T. M. D.; Pearce, J. M. T.; Holmes, E.; Nicholson, J. K. The consortium for metabonomic toxicology (COMET): Aims, activities and achievements. *Pharmacogenomics* **2005**, *6* (7), 691−699.
(17) Schnackenberg, L. K.; Beger, R. D. The role of metabolic biomarkers in drug toxicity studies. *Toxicol. Mech. Methods* **2008**, *18* (4), 301−311.
(18) Robertson, D. G. Metabonomics in toxicology: A review. *Toxicol. Sci.* **2005**, *85* (2), 809−822.
(19) Cantor, G. H.; Beckonert, O.; Bollard, M. E.; Keun, H. C.; Ebbels, T. M. D.; Antti, H.; Wijsman, J. A.; Bible, R. H.; Breau, A. P.; Cockerell, G. L.; Holmes, E.; Lindon, J. C.; Nicholson, J. K. Integrated histopathological and urinary metabonomic investigation of the pathogenesis of microcystin-LR toxicosis. *Vet. Pathol.* **2012**, DOI: 10.1177/0300985812443839.
(20) Schnackenberg, L. K.; Chen, M.; Sun, J.; Holland, R. D.; Dragan, Y.; Tong, W.; Welsh, W.; Beger, R. D. Evaluations of the transsulfuration pathway in multiple liver toxicity studies. *Toxicol. Appl. Pharmacol.* **2009**, *235* (1), 25−32.
(21) Li, G. B. S. Investigation of the effect of exposure to non cytotoxic amounts of microcystins. *Metabolomics* **2011**, *4*, 485−499.
(22) Kondo, F.; Matsumoto, H.; Yamada, S.; Ishikawa, N.; Ito, E.; Nagata, S.; Ueno, Y.; Suzuki, M.; Harada, K.-i. Detection and identification of metabolites of microcystins formed *in vivo* in mouse and rat livers. *Chem. Res. Toxicol.* **1996**, *9* (8), 1355−1359.
(23) Pflugmacher, S.; Wiegand, C.; Oberemm, A.; Beattie, K. A.; Krause, E.; Codd, G. A.; Steinberg, C. E. W. Identification of an enzymatically formed glutathione conjugate of the cyanobacterial hepatotoxin microcystin-LR: The first step of detoxication. *Biochim. Biophys. Acta* **1998**, *1425* (3), 527−533.
(24) Hamadeh, H. K.; Knight, B. L.; Haugen, A. C.; Sieber, S.; Amin, R. P.; Bushel, P. R.; Stoll, R.; Blanchard, K.; Jayadev, S.; Tennant, R. W.; Cunningham, M. L.; Afshari, C. A.; Paules, R. S. Methapyrilene toxicity: Anchorage of pathologic observations to gene expression alterations. *Toxicol. Pathol.* **2002**, *30* (4), 470−482.
(25) Waring, J. F.; Ulrich, R. G.; Flint, N.; Morfitt, D.; Kalkuhl, A.; Staedtler, F.; Lawton, M.; Beekman, J. M.; Suter, L. Interlaboratory evaluation of rat hepatic gene expression changes induced by methapyrilene. *Environ. Health Perspect.* **2004**, *112* (4), 439−448.
(26) Anderson, N. L.; Copple, D. C.; Bendele, R. A.; Probst, G. S.; Richardson, F. C. Covalent protein modifications and gene expression changes in rodent liver following administration of methapyrilene: A study using two-dimensional electrophoresis. *Fundam. Appl. Toxicol.* **1992**, *18* (4), 570−580.
(27) Richardson, F. C.; Strom, S. C.; Copple, D. M.; Bendele, R. A.; Probst, G. S.; Leigh Anderson, N. Comparisons of protein changes in human and rodent hepatocytes induced by the rat-specific carcinogen, methapyrilene. *Electrophoresis* **1993**, *14* (1), 157−161.
(28) Cunningham, M. L.; Pippin, L. L.; Anderson, N. L.; Wenk, M. L. The hepatocarcinogen methapyrilene but not the analog pyrilamine induces sustained hepatocellular replication and protein alterations in F344 rats in a 13-week feed study. *Toxicol. Appl. Pharmacol.* **1995**, *131* (2), 216−223.
(29) Wang, M.; Chan, L. L.; Si, M.; Hong, H.; Wang, D. Proteomic analysis of hepatic tissue of zebrafish (*Danio rerio*) experimentally exposed to chronic microcystin-LR. *Toxicol. Sci.* **2010**, *113* (1), 60−69.
(30) Rogers, E. D.; Henry, T. B.; Twiner, M. J.; Gouffon, J. S.; McPherson, J. T.; Boyer, G. L.; Sayler, G. S.; Wilhelm, S. W. Global gene expression profiling in larval zebrafish exposed to microcystin-LR and microcystis reveals endocrine disrupting effects of cyanobacteria. *Environ. Sci. Technol.* **2011**, *45* (5), 1962−1969.
(31) Imanishi, S.; Harada, K. Proteomics approach on microcystin binding proteins in mouse liver for investigation of microcystin toxicity. *Toxicon* **2004**, *43* (6), 651−659.
(32) Wei, L.; Sun, B.; Song, L.; Nie, P. Gene expression profiles in liver of zebrafish treated with microcystin-LR. *Environ. Toxicol. Pharmacol.* **2008**, *26* (1), 6−12.
(33) Mezhoud, K.; Praseuth, D.; Puiseux-Dao, S.; Francois, J.-C.; Bernard, C.; Edery, M. Global quantitative analysis of protein expression and phosphorylation status in the liver of the medaka fish (*Oryzias latipes*) exposed to microcystin-LR I. Balneation study. *Aquat. Toxicol.* **2008**, *86* (2), 166−175.
(34) Chen, J.; Zhang, D.; Lei, H. In situ studies on the distribution patterns and dynamics of microcystins in a biomanipulation fish - bighead carp (*Aristichthys nobilis*). *Environ. Pollut.* **2007**, *147* (1), 150−157.
(35) Zhang, D.; Xie, P.; Chen, J.; Dai, M.; Qiu, T.; Liu, Y.; Liang, G. Determination of microcystin-LR and its metabolites in snail (*Bellamya aeruginosa*), shrimp (*Macrobrachium nipponensis*) and silver carp (*Hypophthalmichthys molitrix*) from lake Taihu, china. *Chemosphere* **2009**, *76* (7), 974−981.
(36) Botha, N.; Venter, M. v. d.; Downing, T. G.; Shephard, E. G.; Gehringer, M. M. The effect of intraperitoneally administered microcystin-LR on the gastrointestinal tract of balb/c mice. *Toxicon* **2004**, *43* (3), 251−254.
(37) Dai, M.; Xie, P.; Liang, G.; Chen, J.; Lei, H. Simultaneous determination of microcystin-LR and its glutathione conjugate in fish tissues by liquid chromatography-tandem mass spectrometry. *J. Chromatogr., B* **2008**, *862* (1−2), 43−50.
(38) Yoshida, T.; Makita, Y.; Nagata, S.; Tsutsumi, T.; Yoshida, F.; Sekijima, M.; Tamura, S.-i.; Ueno, Y. Acute oral toxicity of microcystin-LR, a cyanobacterial hepatotoxin, in mice. *Nat. Toxins* **1997**, *5* (3), 91−95.
(39) Fawell, J. K.; Mitchell, R. E.; Everett, D. J.; Hill, R. E. The toxicity of cyanobacterial toxins in the mouse: I microcystin-LR. *Hum. Exp. Toxicol.* **1999**, *18* (3), 162−167.
(40) Wu, J.; An, Y.; Yao, J.; Wang, Y.; Tang, H. An optimized sample preparation method for NMR-based faecal metabonomic analysis. *Analyst* **2010**, *135* (5), 1023−1030.
(41) Beckonert, O.; Keun, H. C.; Ebbels, T. M. D.; Bundy, J.; Holmes, E.; Lindon, J. C.; Nicholson, J. K. Metabolic profiling, metabolomic and metabonomic procedures for NMR spectroscopy of urine, plasma, serum and tissue extracts. *Nat. Protoc.* **2007**, *2* (11), 2692−2703.
(42) Trygg, J. O2-PLS for qualitative and quantitative analysis in multivariate calibration. *J. Chemom.* **2002**, *16* (6), 283−293.
(43) Trygg, J.; Wold, S. O2-PLS, a two-block (X-Y) latent variable regression (LVR) method with an integral OSC filter. *J. Chemom.* **2003**, *17* (1), 53−64.
(44) Cloarec, O.; Dumas, M. E.; Trygg, J.; Craig, A.; Barton, R. H.; Lindon, J. C.; Nicholson, J. K.; Holmes, E. Evaluation of the orthogonal projection on latent structure model limitations caused by chemical shift variability and improved visualization of biomarker changes in ^{1}H NMR spectroscopic metabonomic studies. *Anal. Chem.* **2005**, *77* (2), 517−526.
(45) Robinson, N. A.; Miura, G. A.; Matson, C. F.; Dinterman, R. E.; Pace, J. G. Characterization of chemically tritiated microcystin-LR and its distribution in mice. *Toxicon* **1989**, *27* (9), 1035−1042.
(46) Naseem, S. M.; Mereish, K. A.; Solow, R.; Hines, H. B. Microcystin-induced activation of prostaglandin synthesis and phospholipid metabolism in rat hepatocytes. *Toxicol. In Vitro* **1991**, *5* (4), 341−345.

(47) Van Apeldoorn, M. E.; Van Egmond, H. P.; Speijers, G. J.; Bakker, G. J. Toxins of cyanobacteria. *Mol. Nutr. Food Res.* **2007**, *51* (1), 7−60.
(48) Wang, Y.; Tang, H.; Holmes, E.; Lindon, J. C.; Turini, M. E.; Sprenger, N.; Bergonzelli, G.; Fay, L. B.; Kochhar, S.; Nicholson, J. K. Biochemical characterization of rat intestine development using high-resolution magic-angle-spinning 1H NMR spectroscopy and multivariate data analysis. *J. Proteome Res.* **2005**, *4* (4), 1324−1329.
(49) Falconer, I. R.; Dornbusch, M.; Moran, G.; Yeung, S. K. Effect of the cyanobacterial (blue-green algal) toxins from microcystis aeruginosa on isolated enterocytes from the chicken small intestine. *Toxicon* **1992**, *30* (7), 790−793.
(50) Dahlem, A. M.; Hassan, A. S.; Swanson, S. P.; Carmichael, W. W.; Beasley, V. R. A model system for studying the bioavailability of intestinally administered microcystin-LR, a hepatotoxic peptide from the cyanobacterium microcystis aeruginosa. *Pharmacol. Toxicol.* **1989**, *64* (2), 177−181.
(51) Ito, E.; Kondo, F.; Harada, K.-I. First report on the distribution of orally administered microcystin-LR in mouse tissue using an immunostaining method. *Toxicon* **2000**, *38* (1), 37−48.
(52) Kuiper-Goodman, T.; Falconer, I. R.; Fitzgerald, J. Human Health Aspects. In *Toxic Cyanobacteria in Water*; Chorus, I., Bartram, J., Eds.; E&FN Spon: London, 1999; pp 113−153.
(53) Moreno, I.; Mate, A.; Repetto, G.; Vázquez, C.; Cameán, A. Influence of microcystin-LR on the activity of membrane enzymes in rat intestinal mucosa. *J. Physiol. Biochem.* **2003**, *59* (4), 293−299.
(54) Elsaadi, O. E.; Esterman, A. J.; Cameron, S.; Roder, D. M. Murray river water, raised cyanobacterial cell counts, and gastrointestinal and dermatological symptoms. *Med. J. Aust.* **1995**, *162* (3), 122−125.
(55) Benage, D.; O'Connor, K. W. Cholecystocolonic fistula: Malabsorptive consequences of lost bile acids. *J. Clin. Gastroenterol.* **1990**, *12* (2), 195−197.
(56) Hofmann, A. F. The continuing importance of bile acids in liver and intestinal disease. *Arch. Intern. Med.* **1999**, *159* (22), 2647−2658.
(57) Holt, P. R. The roles of bile acids during the process of normal fat and cholesterol absorption. *Arch. Intern. Med.* **1972**, *130* (4), 574−583.
(58) Gilbert, H. F. Basic concepts in biochemistry: A student's survival guide. *Biochem. Educ.* **1992**, *20* (3), 186−186.
(59) Malécot, M.; Mezhoud, K.; Marie, A.; Praseuth, D.; Puiseux-Dao, S.; Edery, M. Proteomic study of the effects of microcystin-LR on organelle and membrane proteins in medaka fish liver. *Aquat. Toxicol.* **2009**, *94* (2), 153−161.
(60) Fladmark, K. E.; Brustugun, O. T.; Mellgren, G.; Krakstad, C.; Bøe, R.; Vintermyr, O. K.; Schulman, H.; Døskeland, S. O. Ca2+/calmodulin-dependent protein kinase ii is required for microcystin-induced apoptosis. *J. Biol. Chem.* **2002**, *277* (4), 2804−2811.
(61) Campos, A.; Vasconcelos, V. Molecular mechanisms of microcystin toxicity in animal cells. *Int. J. Mol. Sci.* **2010**, *11* (1), 268−287.
(62) Labelle, Y.; Phaneuf, D.; Leclerc, B.; M.Tanguay, R. Characterization of the human fumarylacetoacetate hydrolase gene and identification of a missense mutation abolishing enzymatic activity. *Hum. Mol. Genet.* **1993**, *2* (7), 941−946.
(63) Dunkley, P. R.; Bobrovskaya, L.; Graham, M. E.; Von Nagy-Felsobuki, E. I.; Dickson, P. W. Tyrosine hydroxylase phosphorylation: Regulation and consequences. *J. Neurochem.* **2004**, *91* (5), 1025−1043.
(64) Leal, R. B.; Sim, A. T. R.; Goncalves, C. A. S.; Dunkley, P. R. Tyrosine hydroxylase dephosphorylation by protein phosphatase 2a in bovine adrenal chromaffin cells. *Neurochem. Res.* **2002**, *27* (3), 207−213.
(65) Nicholson, J. K.; Wilson, I. D. Understanding 'global' systems biology: Metabonomics and the continuum of metabolism. *Nat. Rev. Drug Discovery* **2003**, *2* (8), 668−676.
(66) Dumas, M.-E.; Barton, R. H.; Toye, A.; Cloarec, O.; Blancher, C.; Rothwell, A.; Fearnside, J.; Tatoud, R.; Blanc, V.; Lindon, J. C.; Mitchell, S. C.; Holmes, E.; McCarthy, M. I.; Scott, J.; Gauguier, D.; Nicholson, J. K. Metabolic profiling reveals a contribution of gut microbiota to fatty liver phenotype in insulin-resistant mice. *Proc. Natl. Acad. Sci.* **2006**, *103* (33), 12511−12516.
(67) Al-Waiz, M.; Mikov, M.; Mitchell, S. C.; Smith, R. L. The exogenous origin of trimethylamine in the mouse. *Metabolism* **1992**, *41* (2), 135−136.
(68) Wang, Z.; Klipfell, E.; Bennett, B. J.; Koeth, R.; Levison, B. S.; DuGar, B.; Feldstein, A. E.; Britt, E. B.; Fu, X.; Chung, Y.-M.; Wu, Y.; Schauer, P.; Smith, J. D.; Allayee, H.; Tang, W. H. W.; DiDonato, J. A.; Lusis, A. J.; Hazen, S. L. Gut flora metabolism of phosphatidylcholine promotes cardiovascular disease. *Nature* **2011**, *472* (7341), 57−63.
(69) Dong, C.; Yoon, W.; Goldschmidt-Clermont, P. J. DNA methylation and atherosclerosis. *J. Nutr.* **2002**, *132* (8), 2406S−2409S.
(70) Zaina, S.; Lindholm, M. W.; Lund, G. Nutrition and aberrant DNA methylation patterns in atherosclerosis: More than just hyperhomocysteinemia? *J. Nutr.* **2005**, *135* (1), 5−8.
(71) Martin, F.-P. J.; Dumas, M.-E.; Wang, Y.; Legido-Quigley, C.; Yap, I. K. S.; Tang, H.; Zirah, S.; Murphy, G. M.; Cloarec, O.; Lindon, J. C.; Sprenger, N.; Fay, L. B.; Kochhar, S.; van Bladeren, P.; Holmes, E.; Nicholson, J. K. A top-down systems biology view of microbiome-mammalian metabolic interactions in a mouse model. *Mol. Syst. Biol.* **2007**, 3.
(72) Salmon, W. D.; Newberne, P. M. Cardiovascular disease in choline-deficient rats—Effects of choline deficiency, nature and level of dietary lipids and proteins, and duration of feeding on plasma and liver lipid values and cardiovascular lesions. *Arch. Pathol.* **1962**, *73* (3), 190−209.
(73) Pajares, M.; Pérez-Sala, D. Betaine homocysteine s-methyltransferase: Just a regulator of homocysteine metabolism? *Cell. Mol. Life Sci.* **2006**, *63* (23), 2792−2803.
(74) Kondo, F.; Ikai, Y.; Oka, H.; Okumura, M.; Ishikawa, N.; Harada, K.; Matsuura, K.; Murata, H.; Suzuki, M. Formation, characterization, and toxicity of the glutathione and cysteine conjugates of toxic heptapeptide microcystins. *Chem. Res. Toxicol.* **1992**, *5* (5), 591−596.
(75) Ito, E.; Takai, A.; Kondo, F.; Masui, H.; Imanishi, S.; Harada, K.-i. Comparison of protein phosphatase inhibitory activity and apparent toxicity of microcystins and related compounds. *Toxicon* **2002**, *40* (7), 1017−1025.
(76) He, J.; Chen, J.; Xie, P.; Zhang, D.; Li, G.; Wu, L.; Zhang, W.; Guo, X.; Li, S. Quantitatively evaluating detoxification of the hepatotoxic microcystins through the glutathione and cysteine pathway in the cyanobacteria-eating bighead carp. *Aquat. Toxicol.* **2012**, *116−117* (0), 61−68.
(77) Bouaıcha, N.; Maatouk, I. Microcystin-LR and nodularin induce intracellular glutathione alteration, reactive oxygen species production and lipid peroxidation in primary cultured rat hepatocytes. *Toxicol. Lett.* **2004**, *148* (1−2), 53−63.
(78) Wu, G.; Fang, Y.-Z.; Yang, S.; Lupton, J. R.; Turner, N. D. Glutathione metabolism and its implications for health. *J. Nutr.* **2004**, *134* (3), 489−492.
(79) Mikhailov, A.; Härmälä-Braskén, A.-S.; Hellman, J.; Meriluoto, J.; Eriksson, J. E. Identification of ATP-synthase as a novel intracellular target for microcystin-LR. *Chem.-Biol. Interact.* **2003**, *142* (3), 223−237.
(80) Fawell, J. K.; James, C. P.; James, H. A. Toxins from blue-green algae: Toxicological assessment of microcystin-LR and a method for determination in water. *Water Res. Center, Medmenham, UK* **1994**, 1−46.
(81) Falconer, I. R.; Burch, M. D.; Steffensen, D. A.; Choice, M.; Coverdale, O. R. Toxicity of the blue-green alga (cyanobacterium) microcystis aeruginosa in drinking water to growing pigs, as an animal model for human injury and risk assessment. *Environ. Toxicol. Water Qual.* **1994**, *9* (2), 131−139.
(82) Falconer, I.; Humpage, A. Health risk assessment of cyanobacterial (blue-green algal) toxins in drinking water. *Int. J. Environ. Res. Public Health* **2005**, *2* (1), 43−50.